ISSN 0915-633X

NATIONAL INSTITUTE FOR FUSION SCIENCE

The Energy Broadening Resulting from Electron Stripping Process of a Low Energy Au^- Beam

A. Taniike, M. Sasao, Y. Hamada, J. Fujita, M. Wada

(Received - Nov. 10, 1994)

NIFS-325 Dec. 1994

RESEARCH REPORT
NIFS Series

NAGOYA, JAPAN

The Energy Broadening Resulting from Electron Stripping Process of a Low Energy Au^- Beam

Akira Taniike, Mamiko Sasao[1)], Yasuji Hamada[1)],
Junji Fujita[1)], Motoi Wada[2)]

Department of Fusion Science
The Graduate University for Advanced Studies
Furo-cho, Chikusa-ku, Nagoya, 460-01, Japan
[1)]*National Institute for Fusion Science*
Furo-cho, Chikusa-ku, Nagoya, 460-01, Japan
[2)]*Department of Electronics, Doshisha University,*
Tanabe, Kyoto 610-03, Japan

Abstract

Energy loss spectra of Au^+ ions produced from Au^- ions by electron stripping in He, Ar, Kr and Xe have been measured in the impact energy range of 24-44 keV. The energy broadening of the Au^+ beam increases as the beam energy increases, and the spectrum shows a narrower energy width for heavy target atoms. The dependence of the spectrum width upon the beam energy and that upon the target mass are well described by the calculation based on the unified potential and semi-classical internal energy transfer model of Firsov's.

Keywords: energy broadening, energy loss, negative gold ion beam, positive gold ion beam, tandem acceleration, electron stripping, elastic process, inelastic process, HIBP

§1. Introduction

When a highly collimated ion beam is utilized for practical application, the forward scattering of a beam in a gas is thought to be one of the key problems. Especially, the energy spectra of positive ions produced from negative ions have lately attracted attentions of researchers in accelerator physics. Together with the recent progress on high voltage generators, the development on negative ion sources makes it possible to generate a high intensity and highly collimated beam by the use of a tandem acceleration system. Here a small energy spread is required on the positive beam generated in the charge exchange gas cell on the high voltage terminal [1].

There have been many studies done on the angular distribution and the energy spectrum of the scattered secondary particles in heavy ion collisions at a small impact parameters, and various information on the intrinsic structures of atoms has been obtained [2]. The change of energy spectra of the incident ions resulting from forward angle atomic collisions at a large impact parameter should be also affected by the effective potentials between atoms, and/or atomic excitations.

One of examples of a highly collimated beam generated by a tandem acceleration system is the Heavy Ion Beam Probe (HIBP) for the Large Helical Device (LHD)[3]. The LHD is a magnetically confined fusion plasma device under construction in National Institute for Fusion Science, Japan. A singly charged positive ion beam of gold (Au^+) produced from a Au^- beam with a 3 MV tandem acceleration system, will be used to measure plasma potentials [4]. Here, the energy spread of output beam

must be small enough to measure a plasma potential as small as a few keV.

A tandem acceleration test stand has been constructed in order to measure the charge state fraction, the beam profiles and the beam energy spectrum of Au^+. The energy spectrum has been measured when the charge stripping gas is thin enough so that the two-electron stripping process ($Au^- \rightarrow Au^+$) is dominant and the multiple collision processes are negligible. In the following section, the experimental setup is briefly shown. The theoretical model to treat the energy broadening due to the electron stripping process is described in the section 3. In the section 4, the results of calculation using this model are presented and compared with experimental results. The conclusion is given in the section 5.

§2. Experimental Apparatus

Figure 1a shows a schematic view of the tandem acceleration test stand, which consists of a plasma-sputter-type gold negative ion source, a tandem acceleration system and an energy analyzer [5].

The energy spectrum of negative ions produced from this type of source has been extensively studied [6][7]. It has an average energy of the target bias voltage (typically 300-400 V) plus a few eV, and its full width half maximum (FWHM) is less than several eV. This is confirmed in the present experiment.

The negative ions from the ion source are preaccelerated with an typical energy of 4 keV, and injected into the accelerator column. The stability of the power supply for the preacceleration and that for the tandem acceleration are 1×10^{-4}.

The charge stripping gas cell of a 14 mm diameter and 700 mm length is installed on the high voltage terminal. The cell is contained in a 900 mm length cylinder with an entrance and exit cylindrical tubes of the 14 mm diameter. An inert gas, such as He, Ar, Kr or Xe is introduced into the cell. The gas pressure is directly measured by an ionization gauge near the cell. The effective target thickness is determined by measuring the attenuation cross sections of a H^- beam in an Ar gas target measured at 4, 5 and 7 keV and comparing with those of the empirical fitting curve [8]. It was (70±15) % of the measured gas density times the cell length.

The positive ions produced in the cell are accelerated again to the ground potential and their energy spectra are measured by a 90 degree cylindrical electro-static analyzer (see Fig. 1b). A slit of 0.4 mm at the exit of the accelerator column restricts the beam entrance angle and improves the resolution of the analyzer. Two slits, a 0.015 mm slit at the entrance and a 0.03 mm slit at the exit are set. The two electrodes are biased with the same voltages of opposite polarity. The first power supply generates a fixed voltage, and the second power supply adds variable voltage of ± 100 V. A pair of samarium-cobalt magnets are installed to sweep out the impurity ions in the beam. It was experimentally confirmed that the effect of this magnetic field on the resolution of the analyzer was negligibly small. An energy spectrum is obtained by sweeping the positive and negative bias voltages on the electrodes in every 0.1 V step with a personal computer, and counting the number of pulses from the secondary electron multiplier that detects beam particles passing through the exit slit. Typical spectra of a Au^- beam (a) and a Au^+ beam (b) are shown

in Fig.2. The overall energy resolution was calibrated by analyzing the direct Ar^+ beam from the source, and turned out to be 4.1×10^{-4}.

§3. A Theoretical Model of Energy Transfer during Electron Stripping Process of Negative Heavy Ions at a Forward Angle

The energy loss mechanism of a projectile in collision with a neutral atom can be considered through the elastic and inelastic processes which occurring simultaneously.

The elastic process corresponds to the scattering by the potential between two atoms, whereas, the inelastic process corresponds to that accompanied by a energy transfer into an internal energy, such as electron loss, ionization, and/or excitation of projectile and target atoms.

3.1 *Energy Loss in Elastic Process*

For the elastic energy transfer, classical theory can be used. The scattering angle θ [rad] in center of mass frame is expressed by an impact parameter b , and an impact energy E , as follows,

$$\theta(b,E) = \pi - 2\int_{r_0}^{\infty} \frac{b}{\sqrt{1-\frac{b^2}{r^2}-\frac{V(r)}{E}}}\frac{dr}{r^2} \qquad (1),$$

here, r_0 is the closest distance during the collision, and it is the solution of Eq.2.

$$1-\frac{b^2}{r_0^2}-\frac{V(r_0)}{E}=0 \qquad (2)$$

$V(r)$ is the potential between the two atoms, and here we use the unified potential which was proposed by Ziegler et al. [9].

$$V(r)=\frac{Z^2e^2}{r}\left(\phi_a(r)-Z^{-2/3}\phi_b(r)\right) \qquad (3)$$

$$\phi_a(r)=0.09e^{-0.19x}+0.61e^{-0.57x}+0.3e^{-2x}$$

$$\phi_b(r)=0.07\exp\left\{-\left(\frac{1}{7R}\right)^2-\frac{R}{4}-\left(\frac{R}{4}\right)^2\right\}$$

where,

$$x=R/a\ ,\quad a=0.8853a_0Z^{-1/3}\ ,\quad R=Z^{1/3}r,$$

a_0 : Bohr radius.

When Z number of the two atoms are different, the effective potential is

$$V_{12}(r)=\sqrt{V_1(r)V_2(r)} \qquad (4).$$

This potential gives good approximation for large Z atoms. The energy loss T_{el} by elastic process can be expressed,

$$T_{el}(\theta)=T_m\sin^2\left(\frac{\theta}{2}\right) \qquad (5)$$

where T_m is the maximum energy transfer from the projectile to the target atom,

$$T_m=\frac{4M_1M_2}{(M_1+M_2)^2}E \qquad (6)$$

M_1 : mass number of the projectile

M_2 : mass number of the target atom.

The largest scattering angle observed in the experiment, θ_{max}, is limited by the apparatus geometry. The minimum impact parameter, b_{min}, is determined from this angle θ_{max}.

3.2 *Energy Loss in Inelastic Process*

During the inelastic process, a part of the kinetic energy is transferred into an internal energy of projectile and target atoms. The minimum energy required to produce a Au^+ ion from a Au^- ion is a sum of the electron affinity and the first ionization potential of a Au atom.

$$T_{in(Au^- \rightarrow Au^+)} = T_{in,\min} = 11.5 \quad [\text{eV}] \qquad (7)$$

Firsov proposed a theoretical model to describe an inelastic energy transfer [10] , which can be expressed as a function of an impact parameter b [Å] and velocity v [cm/s],

$$T_{in}(b,\mathrm{v}) = \frac{(Z_1 + Z_2)^{5/3} \cdot 4.3 \times 10^{-8}\,\mathrm{v}}{\left[1 + 0.31(Z_1 + Z_2)^{1/3} \cdot b\right]^5} \quad [\text{eV}] \qquad (8)$$

where

Z_1 : atomic number of the projectile

Z_2 : atomic number of the target atom,

under the condition of

$$\frac{1}{4} \le \frac{Z_1}{Z_2} \le 4 \qquad (9).$$

In this model, the two-electron stripping process can occur when

$$T_{in}(b) \ge T_{in(Au^- \rightarrow Au^+)}$$

by which the maximum impact parameter b_{max} is determined.

$$T_{in(Au^- \rightarrow Au^+)} = T_{in}(b_{\max})$$

3.3 *Total Energy Transfer and Energy Broadening*

The amount of energy loss due to elastic and inelastic processes depends upon the impact parameter. The sum of elastic and inelastic energy losses causes the energy broadening of a Au^+ beam.

$$T_{tot}(b) = T_{el}(b) + T_{in}(b)$$

Figure 3 shows the elastic scattering angle θ [rad] in the center of mass system, the elastic energy loss T_{el} [eV] and the inelastic energy loss T_{in} [eV] as a function of impact parameter b [Å], when an Au^- ion is injected with an impact energy of 44 keV into the Ar target. The elastic energy loss T_{el} dose not affect the energy broadening in the energy range of the present experiment.

The energy spectrum which is observed in the experiment can be expressed as

$$F(\varepsilon)=2\pi\cdot b(\varepsilon)\cdot f(\theta) \quad ,$$

where the $b\,(\varepsilon)$ is the inverse function of $T\,(b)$, and $f(\theta)$ is the efficiency of particle detection for the present experimental system. The latter is also a function of an impact parameter, which becomes zero at $b=b_{min}$ (or $\theta=\theta_{max}$). As a measure to compare with the experimental results, here we consider an impact parameter $b_{1/2}$ and an energy transfer $T_{tot}\,(b_{1/2})$ as the following,

$$b_{1/2}=\frac{(b_{\max}+b_{\min})}{2}$$

$$T_{tot}(b_{1/2})=T_{el}(b_{1/2})+T_{in}(b_{1/2})-11.5 \quad \text{[eV]}.$$

In Fig.4. are shown the energy loss $T_{tot}\,(b_{1/2})$ as a function of impact energy E [keV] in He, Ne, Ar, Kr and Xe , where $b_{1/2}$ is a half value of the observable impact parameter. The $T_{tot}\,(b_{1/2})$ increases as an impact energy increases, and it is larger for light target atoms.

§4. Experimental Results and Discussion

As is shown in Fig.2, the spectrum of the two-electron stripped Au^+ shows a broader peak than that of the original Au^- beam. Here we call the value of FWHM of this peak as an energy width. The energy width is constant in the region of the target gas thickness less than 2×10^{15} cm^{-2}, and it is broadened by multiple collision at a larger gas thickness. In the present paper, we deal with widths in the region where the multiple collision processes are negligible. We also measured the attenuation curve of the Au^- beam, and selected a gas thickness region where the two-electron stripping process($Au^- \rightarrow Au^+$) was dominant.

Several kinds of inert gases, He, Ar, Kr and Xe were introduced into the stripping cell as the target gas. Figure 5 shows the energy width, as a function of an impact beam energy for those gases when its thickness is smaller than 2×10^{15} cm^{-2}.

The dependence of the energy width upon an impact energy and that upon the target mass show the tendencies as the theoretical prediction. In order to compare them, the calculated energy spectra are convoluted with energy resolution of the analyzer. The result is shown in Fig.5, here, the experimental data points are the measured FWHM before the corection of the resolution. The energy dependence and that upon the target mass are well reproduced and the absolute values are close each other.

Because the scattering angle is a steep increasing function for decreasing impact parameter, the increase of the observation solid angle should not severely affect the spectrum. Especially, the peak shape is mostly determined by the inelastic energy loss near b_{max}. Some discrepancies are seen in comparisons of the measured energy width with the theoretical prediction. The discrepancy in case of He target, might be due to the unsatisfactory condition of Firsov's theory (see Eq.9). The inelastic energy transfer model of Firsov uses an electron distribution function of the semi-classical Thomas-Fermi model. This model is widely accepted to describe an overall structure of collisions between heavy particles at low velocity, but the modification of electron distribution function in an atom might affect the shape of $T(b)$.

§5. Conclusions

Energy broadening due to the two-electron stripping process of gold ions ($Au^- \rightarrow Au^+$) in He, Ar, Kr and Xe is

measured at a forward angle in the impact energy range of 24-44 keV. The FWHM are typically 20-80 eV, and they increase as the impact energy increases. Stripping with low Z target atoms results in a broader energy width. In order to explain the measured energy dependence and the target mass dependence of the spectrum widths, a simple model using the semi-classical internal energy transfer function of Firsov's, and the scattering by the unified potential is proposed. Theoretical prediction of the present model reproduces the energy and mass dependencies of the broadening. The absolute values of the theoretically predicted width are close to the observed FWHM.

Applying the present theoretical prediction to estimate the energy width of the 6 MeV Au^+ beam generated by a tandem acceleration system on LHD, the energy broadening due to the electron stripping will be less than 100 eV. If the pressure of the stripping gas cell is well controlled to avoid multiple collision processes, the energy spread will be small enough for the measurement of a plasma potential of a few keV.

Acknowledgments

The authors greatly appreciate discussions with Drs. H.Tawara,H.Yamaoka, H.Iguchi, and A. Fujisawa, and their helpful comments.

References

[1] A. Taniike, M. Sasao, A. Fujisawa, H. Iguchi, Y. Hamada, J. Fujita, M. Wada and Y. Mori, IEEE Transactions on Plasma Science, Vol. 22, No.4, August 1994.

[2] H. S. W. Massey and H. B. Gilbody, "Electronic and Ionic Impact Phenomena IV", Sec. 24, (1974, Oxford Press)

[3] O.Motojima, et al., In Plasma Physics and Controlled Nuclear Fusion Research 1990 (proc. 13th Int. Conf. Washington, 1990), IAEA-CN-53/G-I-5, 513 (1990).

[4] A.Fujisawa, H.Iguchi, Y.Hamada, M.Sasao, J.Fujita, Rev. of Sci. Instrum. Vol.63, 3694 (1992).

[5] A.Taniike, Ph. D. thesis (in preparation)

[6] Y.Okabe, M.Sasao, H.Yamaoka, M.Wada and J.Fujita, Jpn. J. Appl. Phys. Vol.30, 1428 (1991).

[7] Y.Okabe, M.Sasao, H.Yamaoka, M.Wada and J.Fujita, Jpn. J. Appl. Phys. Vol.30, 1307 (1991).

[8] N. Andersen, T. Andersen, L. Jepsen and J. Macek, J. Phys. B: At. Mol. Phys. 17, 2281 (1984).

[9] J.P.Biersack and J.F.Ziegler, Nucl. Inst. Meth. 194, 93 (1982).

[10] O.B.Firsov, Soviet Phys. JETP 9, 1076 (1959).
P.Hvelplund, K. Dan. Vid. Selsk. Mat. Fys. Medd. 38, no.4 (1971).

Figure Captions

Fig.1. The schematic view of the tandem acceleration test stand (a). Negative ions extracted from a plasma-sputter-type negative ion source are injected in to the tandem acceleration system, and converted into positive ions in a gas cell on the high voltage terminal. Positive ions are accelerated again to the ground potential and analyzed with a cylindrical energy analyzer (b).

Fig.2. Typical spectra of (a) the original Au^- beam, and (b) the Au^+ beam from the tandem acceleration system. An Ar gas of 2.3×10^{-3} Torr was introduced to the charge stripping cell. The preacceleration and tandem acceleration voltages were 4 kV, and 35 kV, respectively. Here, one channel corresponds to 1.04 eV. The oxygen component has the same energy as the gold beam, but it is swept by the magnets by 30 channels (O^-), or by 80 channels (O^+).

Fig.3. Elastic scattering angle θ [rad] in the center of mass system, the elastic energy loss T_{el} [eV] and the inelastic energy loss T_{in} [eV] plotted as functions of impact parameter b [Å], when an Au^- ion is injected with an impact energy of 44 keV, into the Ar target to produce a Au^+ ion beam. The elastic scattering angle and energy loss are calculated by classical theory with Ziegler's unified potential between two atoms, the inelastic energy loss is calculated by Firsov's theory. A θ_{max} is largest observable angle in center of mass coordinate determined by experimental geometry.

Fig.4. The numerically calculated energy losses, $T_{tot}(b_{1/2})$, plotted as functions of impact energy, E [keV], for target gases He, Ne, Ar, Kr and Xe. The impact parameter $b_{1/2}$ is a mean of b_{min} and b_{max}.

Fig.5. The dependence of the measured energy width on the impact energy, for target gases of He, Ar, Kr and Xe. Solid curves indicate the calculated energy width of $T_{tot}(b_{1/2})$ (Fig.2.) convoluted by the energy resolution of the analyzer.

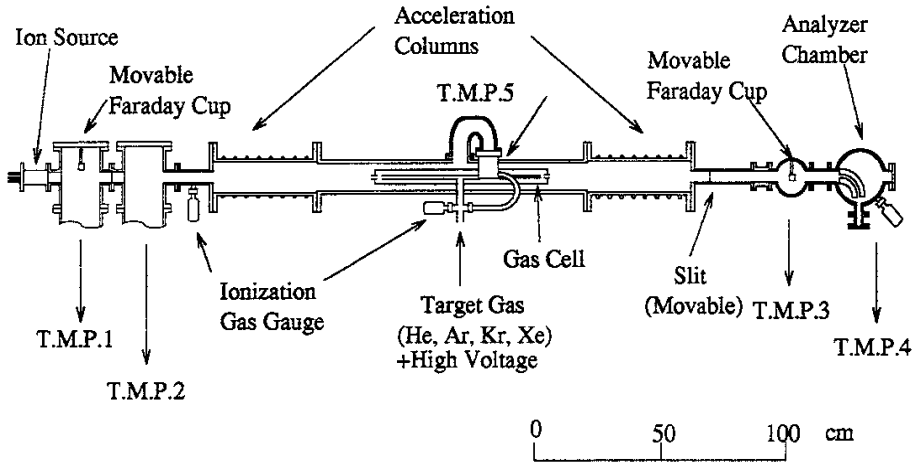

(a)

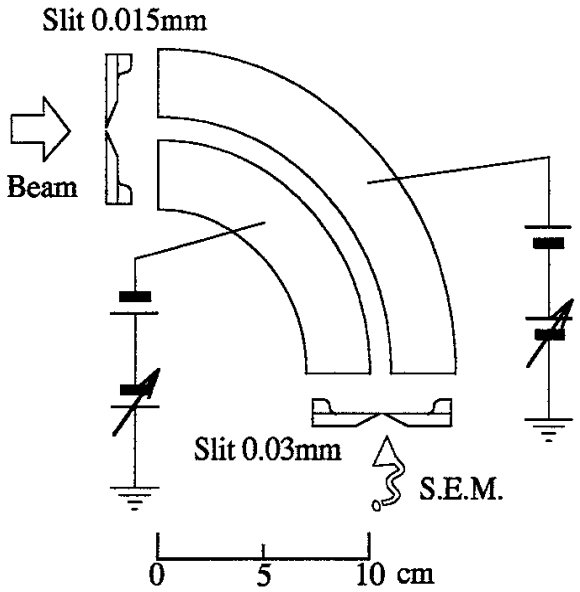

(b)

Fig.1. The schematic view of the tandem acceleration test stand (a). Negative ions extracted from a plasma-sputter-type negative ion source are injected in to the tandem acceleration system, and converted into positive ions in a gas cell on the high voltage terminal. Positive ions are accelerated again to the ground potential and analyzed with a cylindrical energy analyzer (b).

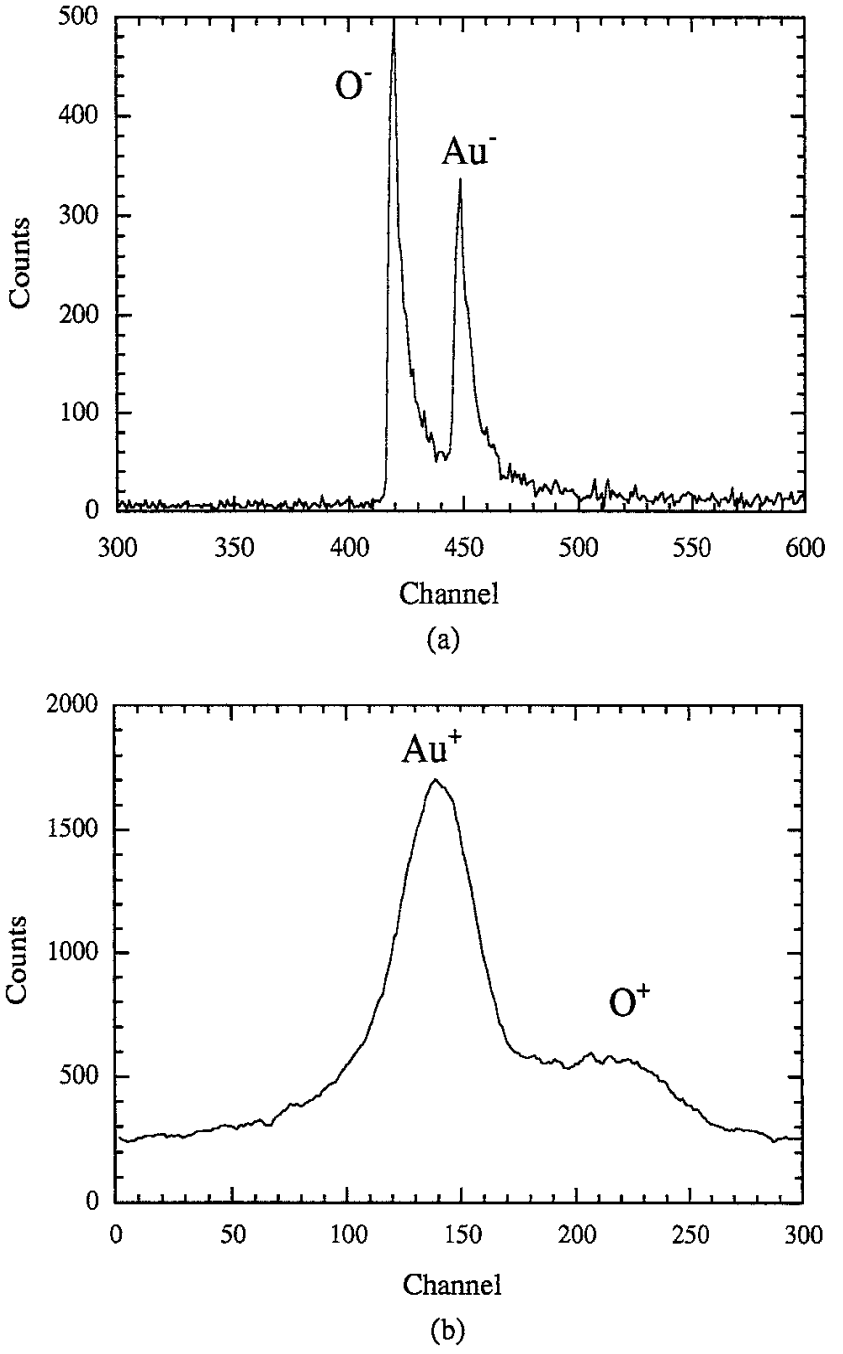

Fig.2. Typical spectra of (a) the original Au^- beam, and (b) the Au^+ beam from the tandem acceleration system. An Ar gas of 2.3×10^{-3} Torr was introduced to the charge stripping cell. The preacceleration and tandem acceleration voltages were 4 kV, and 35 kV, respectively. Here, one channel corresponds to 1.04 eV. The oxygen component has the same energy as the gold beam, but it is swept by the magnets by 30 channels (O^-), or by 80 channels (O^+).

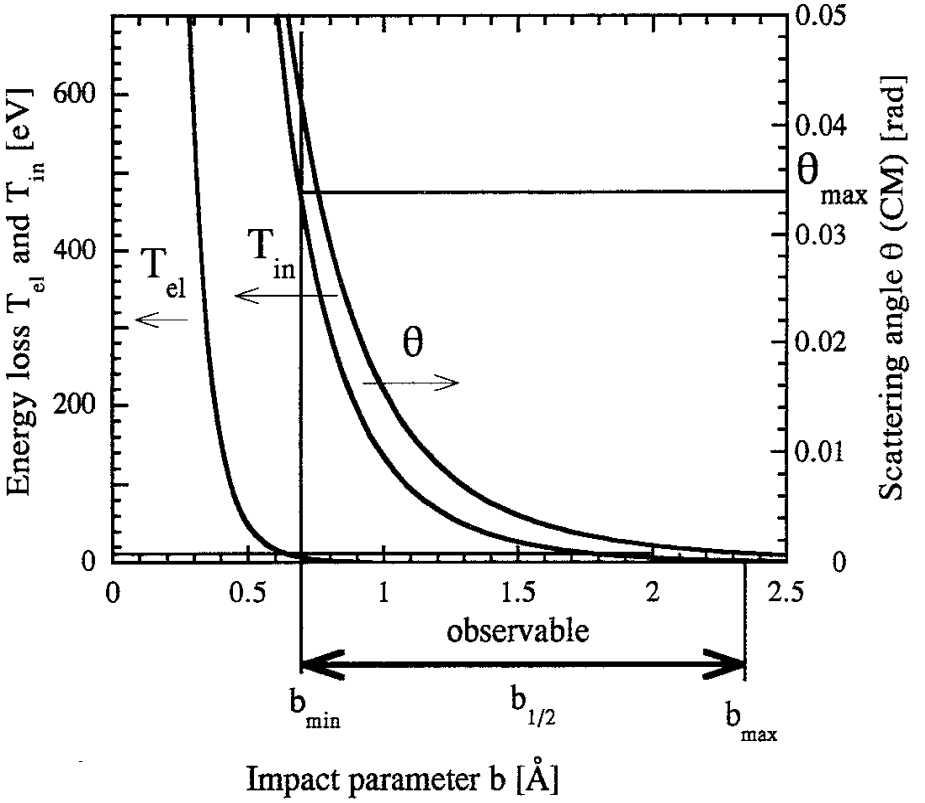

Fig.3. Elastic scattering angle θ [rad] in the center of mass system, the elastic energy loss T_{el} [eV] and the inelastic energy loss T_{in} [eV] plotted as functions of impact parameter b [Å], when an Au^- ion is injected with an impact energy of 44 keV, into the Ar target to produce a Au^+ ion beam. The elastic scattering angle and energy loss are calculated by classical theory with Ziegler's unified potential between two atoms, the inelastic energy loss is calculated by Firsov's theory. A θ_{max} is largest observable angle in center of mass coordinate determined by experimental geometry.

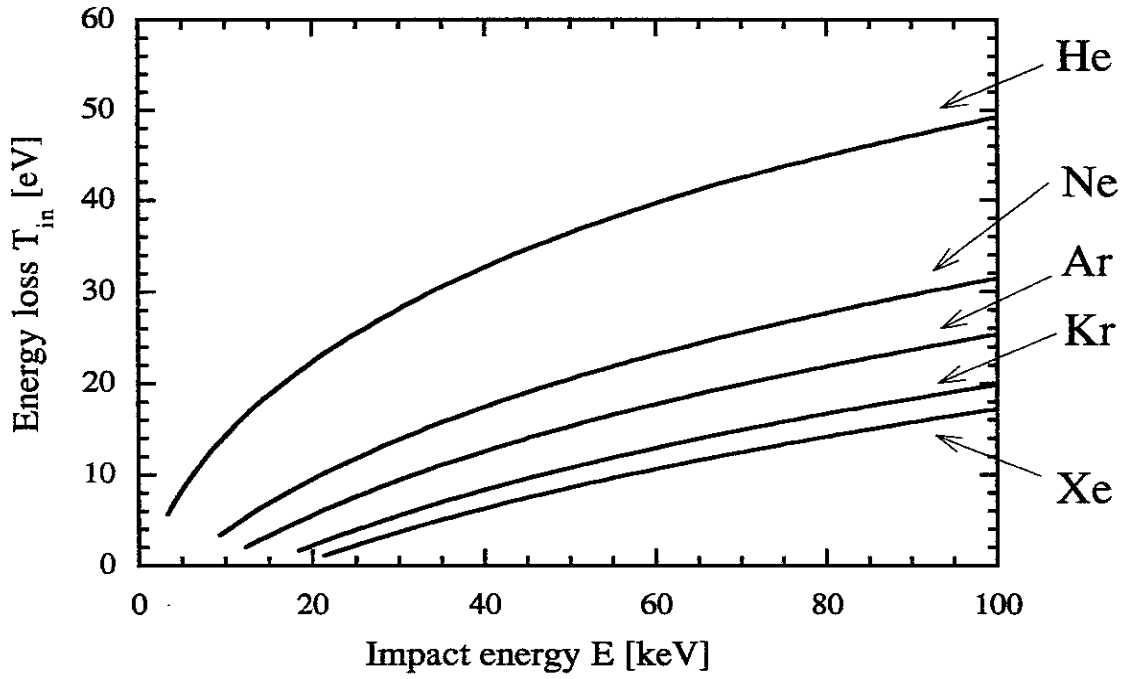

Fig.4. The numerically calculated energy losses, T_{tot} ($b_{1/2}$), plotted as functions of impact energy, E [keV], for target gases He, Ne, Ar, Kr and Xe. The impact parameter $b_{1/2}$ is a mean of b_{min} and b_{max}.

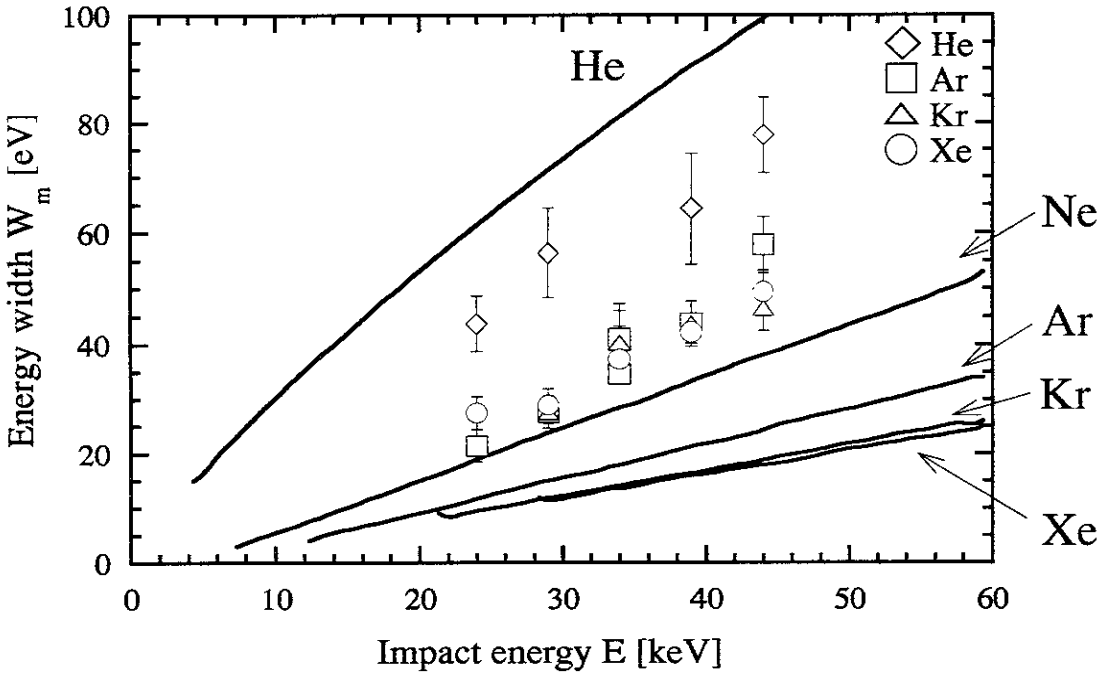

Fig.5. The dependence of the measured energy width on the impact energy, for target gases of He, Ar, Kr and Xe. Solid curves indicate the calculated energy width of T_{tot} ($b_{1/2}$) (Fig.2.) convoluted by the energy resolution of the analyzer.

Recent Issues of NIFS Series

NIFS-284 R. Horiuchi and T. Sato,
Particle Simulation Study of Driven Magnetic Reconnection in a Collisionless Plasma; June 1994

NIFS-285 K.Y. Watanabe, N. Nakajima, M. Okamoto, K. Yamazaki, Y. Nakamura, M. Wakatani,
Effect of Collisionality and Radial Electric Field on Bootstrap Current in LHD (Large Helical Device); June 1994

NIFS-286 H. Sanuki, K. Itoh, J. Todoroki, K. Ida, H. Idei, H. Iguchi and H. Yamada,
Theoretical and Experimental Studies on Electric Field and Confinement in Helical Systems; June 1994

NIFS-287 K. Itoh and S-I. Itoh,
Influence of the Wall Material on the H-mode Performance; June 1994

NIFS-288 K. Itoh, A. Fukuyama, S.-I. Itoh, M. Yagi and M. Azumi,
Self-Sustained Magnetic Braiding in Toroidal Plasmas: July 1994

NIFS-289 Y. Nejoh,
Relativistic Effects on Large Amplitude Nonlinear Langmuir Waves in a Two-Fluid Plasma; July 1994

NIFS-290 N. Ohyabu, A. Komori, K. Akaishi, N. Inoue, Y. Kubota, A.I. Livshit, N. Noda, A. Sagara, H. Suzuki, T. Watanabe, O. Motojima, M. Fujiwara, A. Iiyoshi,
Innovative Divertor Concepts for LHD; July 1994

NIFS-291 H. Idei, K. Ida, H. Sanuki, S. Kubo, H. Yamada, H. Iguchi, S. Morita, S. Okamura, R. Akiyama, H. Arimoto, K. Matsuoka, K. Nishimura, K. Ohkubo, C. Takahashi, Y. Takita, K. Toi, K. Tsumori and I. Yamada,
Formation of Positive Radial Electric Field by Electron Cyclotron Heating in Compact Helical System; July 1994

NIFS-292 N. Noda, A. Sagara, H. Yamada, Y. Kubota, N. Inoue, K. Akaishi, O. Motojima, K. Iwamoto, M. Hashiba, I. Fujita, T. Hino, T. Yamashina, K. Okazaki, J. Rice, M. Yamage, H. Toyoda and H. Sugai,
Boronization Study for Application to Large Helical Device; July 1994

NIFS-293 Y. Ueda, T. Tanabe, V. Philipps, L. Könen, A. Pospieszczyk, U. Samm, B. Schweer, B. Unterberg, M. Wada, N. Hawkes and N. Noda,
Effects of Impurities Released from High Z Test Limiter on Plasma Performance in TEXTOR; July. 1994

NIFS-294 K. Akaishi, Y. Kubota, K. Ezaki and O. Motojima,
Experimental Study on Scaling Law of Outgassing Rate with A Pumping

Parameter, Aug. 1994

NIFS-295 S. Bazdenkov, T. Sato, R. Horiuchi, K. Watanabe,
Magnetic Mirror Effect as a Trigger of Collisionless Magnetic Reconnection, Aug. 1994

NIFS-296 K. Itoh, M. Yagi, S.-I. Itoh, A. Fukuyama, H. Sanuki, M. Azumi,
Anomalous Transport Theory for Toroidal Helical Plasmas,
Aug. 1994 (IAEA-CN-60/D-III-3)

NIFS-297 J. Yamamoto, O. Motojima, T. Mito, K. Takahata, N. Yanagi, S. Yamada, H. Chikaraishi, S. Imagawa, A. Iwamoto, H. Kaneko, A. Nishimura, S. Satoh, T. Satow, H. Tamura, S. Yamaguchi, K. Yamazaki, M. Fujiwara, A. Iiyoshi and LHD group,
New Evaluation Method of Superconductor Characteristics for Realizing the Large Helical Device; Aug. 1994 (IAEA-CN-60/F-P-3)

NIFS-298 A. Komori, N. Ohyabu, T. Watanabe, H. Suzuki, A. Sagara, N. Noda, K. Akaishi, N. Inoue, Y. Kubota, O Motojima, M. Fujiwara and A. Iiyoshi,
Local Island Divertor Concept for LHD; Aug. 1994 (IAEA-CN-60/F-P-4)

NIFS-299 K. Toi, T. Morisaki, S. Sakakibara, A. Ejiri, H. Yamada, S. Morita, K. Tanaka, N. Nakajima, S. Okamura, H. Iguchi, K. Ida, K. Tsumori, S. Ohdachi, K. Nishimura, K. Matsuoka, J. Xu, I. Yamada, T. Minami, K. Narihara, R. Akiyama, A. Ando, H. Arimoto, A. Fujisawa, M. Fujiwara, H. Idei, O. Kaneko, K. Kawahata, A. Komori, S. Kubo, R. Kumazawa, T. Ozaki, A. Sagara, C. Takahashi, Y. Takita and T. Watari,
Impact of Rotational-Transform Profile Control on Plasma Confinement and Stability in CHS; Aug. 1994 (IAEA-CN-60/A6/C-P-3)

NIFS-300 H. Sugama and W. Horton,
Dynamical Model of Pressure-Gradient-Driven Turbulence and Shear Flow Generation in L-H Transition; Aug. 1994 (IAEA/CN-60/D-P-I-11)

NIFS-301 Y. Hamada, A. Nishizawa, Y. Kawasumi, K.N. Sato, H. Sakakita, R. Liang, K. Kawahata, A. Ejiri, K. Narihara, K. Sato, T. Seki, K. Toi, K. Itoh, H. Iguchi, A. Fujisawa, K. Adachi, S. Hidekuma, S. Hirokura, K. Ida, M. Kojima, J. Koog, R. Kumazawa, H. Kuramoto, T. Minami, I. Negi, S. Ohdachi, M. Sasao, T. Tsuzuki, J. Xu, I. Yamada, T. Watari,
Study of Turbulence and Plasma Potential in JIPP T-IIU Tokamak;
Aug. 1994 (IAEA/CN-60/A-2-III-5)

NIFS-302 K. Nishimura, R. Kumazawa, T. Mutoh, T. Watari, T. Seki, A. Ando, S. Masuda, F. Shinpo, S. Murakami, S. Okamura, H. Yamada, K. Matsuoka, S. Morita, T. Ozaki, K. Ida, H. Iguchi, I. Yamada, A. Ejiri, H. Idei, S. Muto, K. Tanaka, J. Xu, R. Akiyama, H. Arimoto, M. Isobe, M. Iwase, O. Kaneko, S. Kubo, T. Kawamoto, A. Lazaros, T. Morisaki, S. Sakakibara, Y. Takita, C. Takahashi and K. Tsumori,
ICRF Heating in CHS; Sep. 1994 (IAEA-CN-60/A-6-I-4)

NIFS-303 S. Okamura, K. Matsuoka, K. Nishimura, K. Tsumori, R. Akiyama, S. Sakakibara, H. Yamada, S. Morita, T. Morisaki, N. Nakajima, K. Tanaka, J. Xu, K. Ida, H. Iguchi, A. Lazaros, T. Ozaki, H. Arimoto, A. Ejiri, M. Fujiwara, H. Idei, A. Iiyoshi, O, Kaneko, K. Kawahata, T. Kawamoto, S. Kubo, T. Kuroda, O. Motojima, V.D. Pustovitov, A. Sagara, C. Takahashi, K. Toi and I. Yamada,
High Beta Experiments in CHS; Sep. 1994 (IAEA-CN-60/A-2-IV-3)

NIFS-304 K. Ida, H. Idei, H. Sanuki, K. Itoh, J. Xu, S. Hidekuma, K. Kondo, A. Sahara, H. Zushi, S.-I. Itoh, A. Fukuyama, K. Adati, R. Akiyama, S. Bessho, A. Ejiri, A. Fujisawa, M. Fujiwara, Y. Hamada, S. Hirokura, H. Iguchi, O. Kaneko, K. Kawahata, Y. Kawasumi, M. Kojima, S. Kubo, H. Kuramoto, A. Lazaros, R. Liang, K. Matsuoka, T. Minami, T. Mizuuchi, T. Morisaki, S. Morita, K. Nagasaki, K. Narihara, K. Nishimura, A. Nishizawa, T. Obiki, H. Okada, S. Okamura, T. Ozaki, S. Sakakibara, H. Sakakita, A. Sagara, F. Sano, M. Sasao, K. Sato, K.N. Sato, T. Saeki, S. Sudo, C. Takahashi, K. Tanaka, K. Tsumori, H.Yamada, I. Yamada, Y. Takita, T. Tuzuki, K. Toi and T. Watari,
Control of Radial Electric Field in Torus Plasma; Sep. 1994
(IAEA-CN-60/A-2-IV-2)

NIFS-305 T. Hayashi, T. Sato, N. Nakajima, K. Ichiguchi, P. Merkel, J. Nührenberg, U. Schwenn, H. Gardner, A. Bhattacharjee and C.C.Hegna,
Behavior of Magnetic Islands in 3D MHD Equilibria of Helical Devices;
Sep. 1994 (IAEA-CN-60/D-2-II-4)

NIFS-306 S. Murakami, M. Okamoto, N. Nakajima, K.Y. Watanabe, T. Watari, T. Mutoh, R. Kumazawa and T. Seki,
Monte Carlo Simulation for ICRF Heating in Heliotron/Torsatrons;
Sep. 1994 (IAEA-CN-60/D-P-I-14)

NIFS-307 Y. Takeiri, A. Ando, O. Kaneko, Y. Oka, K. Tsumori, R. Akiyama, E. Asano, T. Kawamoto, T. Kuroda, M. Tanaka and H. Kawakami,
Development of an Intense Negative Hydrogen Ion Source with a Wide-Range of External Magnetic Filter Field; Sep. 1994

NIFS-308 T. Hayashi, T. Sato, H.J. Gardner and J.D. Meiss,
Evolution of Magnetic Islands in a Heliac; Sep. 1994

NIFS-309 H. Amo, T. Sato and A. Kageyama,
Intermittent Energy Bursts and Recurrent Topological Change of a Twisting Magnetic Flux Tube; Sep.1994

NIFS-310 T. Yamagishi and H. Sanuki,
Effect of Anomalous Plasma Transport on Radial Electric Field in Torsatron/Heliotron; Sep. 1994

NIFS-311 K. Watanabe, T. Sato and Y. Nakayama,
Current-profile Flattening and Hot Core Shift due to the Nonlinear Development of Resistive Kink Mode; Oct. 1994

NIFS-312 M. Salimullah, B. Dasgupta, K. Watanabe and T. Sato,
Modification and Damping of Alfvén Waves in a Magnetized Dusty Plasma; Oct. 1994

NIFS-313 K. Ida, Y. Miura, S -I. Itoh, J.V. Hofmann, A. Fukuyama, S. Hidekuma, H. Sanuki, H. Idei, H. Yamada, H. Iguchi, K. Itoh,
Physical Mechanism Determining the Radial Electric Field and its Radial Structure in a Toroidal Plasma; Oct. 1994

NIFS-314 Shao-ping Zhu, R. Horiuchi, T. Sato and The Complexity Simulation Group,
Non-Taylor Magnetohydrodynamic Self-Organization; Oct. 1994

NIFS-315 M. Tanaka,
Collisionless Magnetic Reconnection Associated with Coalescence of Flux Bundles; Nov. 1994

NIFS-316 M. Tanaka,
Macro-EM Particle Simulation Method and A Study of Collisionless Magnetic Reconnection; Nov. 1994

NIFS-317 A. Fujisawa, H. Iguchi, M. Sasao and Y. Hamada,
Second Order Focusing Property of 210° Cylindrical Energy Analyzer; Nov. 1994

NIFS-318 T. Sato and Complexity Simulation Group,
Complexity in Plasma - A Grand View of Self- Organization; Nov. 1994

NIFS-319 Y. Todo, T. Sato, K. Watanabe, T.H. Watanabe and R. Horiuchi,
MHD-Vlasov Simulation of the Toroidal Alfvén Eigenmode; Nov. 1994

NIFS-320 A. Kageyama, T. Sato and The Complexity Simulation Group,
Computer Simulation of a Magnetohydrodynamic Dynamo II: Nov. 1994

NIFS-321 A. Bhattacharjee, T. Hayashi, C.C.Hegna, N. Nakajima and T. Sato,
Theory of Pressure-induced Islands and Self-healing in Three-dimensional Toroidal Magnetohydrodynamic Equilibria; Nov. 1994

NIFS-322 A. Iiyoshi, K. Yamazaki and the LHD Group,
Recent Studies of the Large Helical Device; Nov. 1994

NIFS-323 A. Iiyoshi and K. Yamazaki,
The Next Large Helical Devices; Nov. 1994

NIFS-324 V.D. Pustovitov
Quasisymmetry Equations for Conventional Stellarators; Nov. 1994